www.czasopisma.pan.pl PAN POLSKA AKADEMIA NAUK www.journals.pan.pl

Arch. Metall. Mater., Vol. 61 (2016), No 3, p. 1607–1612

DOI: 10.1515/amm-2016-0262

A. RADZISZEWSKA*,#, A. KRANZMANN**, I. DÖRFEL**, M. MOSQUERA FEIJOO**, M. SOLECKA*

MICROSTRUCTURE AND CHEMICAL COMPOSITION OF Fe-Cr ALLOY TEMPERED IN HIGH TEMPERATURE AND ATMOSPHERE CONTAINING Ar-SO_2

The paper presents the microstructure, chemical and phase composition of thin scale, obtained as a result of high-temperature corrosion of X20Cr13 stainless steel. Samples were exposed to gas atmosphere of the following composition: 0.25 vol.% of SO_2 and 99.75 vol.% of Ar at 600 °C for 5 h. As a consequence, thin compact scale was formed on steel surface. This scale consisted of three different zones. An amorphous zone was formed close to steel surface. Then, nanocrystalline zone could be observed. Finally, larger grains were formed during the corrosion process. The analysis of the chemical composition revealed higher concentration of chromium near steel surface. In contrast, to chromium, the content of iron, increased near the scale surface. It was found out that the $(Cr, Mn, Fe)_5O_{12}$ phase appeared in the thin scale.

Keywords: Microstructure; High-temperature corrosion; X20Cr13 steel

1. Introduction

The resistance of materials to high-temperature oxidation as well as, in some cases, their resistance to erosion or erosion-corrosion is very important. Therefore, such materials can be applied in energy conversion systems. Materials that comply with these requirements are steels with high content of chromium (e.g. X20Cr13-1.4021) [1-5]. These steels are widely implemented to manufacture elements used in power plants [6-7] and they are characterized by high resistance to harmful impact of environmental factors [8]. Therefore, they are very often applied as injection pipes, shafts, piping designed to transport gasses from combustion processes [9]. When such metallic materials are exposed to the impact of destructive environment, corrosion scales form on their surface. However, heat-resistant alloys, based on Co, Ni and Fe form a protective oxide layer and show good resistance to high-temperature oxidation. It is worth noting that these layers are not entirely protective in the sulphur-oxygen atmospheres. In these sulphur atmospheres and in combustion gases, that contain low amounts of sulphur, the materials exposed to high temperatures undergo very rapid degradation, followed by failure of the devices made of these materials [10-12]. It should be noted that the the degradation rate is higher in the gases containing sulphur than in oxygen environments. This is due to the concentration of defects in metal sulphides, which is many times higher than in oxides [13]. Additionally, compared to the oxide system, they form a low-temperature eutectic in the sulphide system. Therefore, catastrophic corrosion take place in the atmospheres which contain SO_2. Corrosion caused by an atmosphere consisting of sulphur compounds occurs very often and it combines with oxygen corrosion and complicates the course of material degradation. Depending on the type of corrosive environments, the scale may contain oxides, sulphides (e.g. $Fe_{1-x}S$, where $0<x<1$) and spinel of steels components (e.g. $Fe_{1-x}Cr_xS$) [14-15]. Sulphides and metal oxides occur because of the reaction between metal and products of SO_2 dissociation. Therefore, the reaction products are stable and depend on the process conditions and on particular oxygen and sulphur partial pressures in the gas phase [12-13, 15]. However, sulphides could be stable because sulphur partial pressure is higher than the equilibrium sulphur pressure [13]. As can be seen, the corrosion process of alloys in severe multicomponent gas atmospheres is very complicated and still requires extensive research work [16-17].

The present work defines the early stages of corrosion by examining microstructure and chemical composition of the layer formed after high-temperature corrosion of X20Cr13 steel. Very important issues of these investigations the beginning of nucleation and the growth of corroded layer are very important issues, which these investigations are focused on. This required, microstructure and chemical composition to be identified by the scanning and transmission electron microscopy (SEM, TEM) and the energy dispersive spectroscopy (EDS). The phase identification was performed with the fast Fourier transform (FFT).

2. Material and experiment procedure

The examined material was X20Cr13 steel (1.4021) (TABLE 1). The steel samples were exposed to a specific synthetic environment saturated with the technical mixture of 0.25 vol.% SO_2 and 99.75 vol.% Ar at a flow rate >0.01 m/s and at 600 °C for 5 h. The experiments relate to the early stages of stainless steel corrosion.

* AGH UNIVERSITY OF SCIENCE AND TECHNOLOGY 1FACULTY OF METALS ENGINEERING AND INDUSTRIAL COMPUTER SCIENCE, KRAKOW, POLAND

** BAM FEDERAL INSTITUTE FOR MATERIALS RESEARCH AND TESTING, DEPARTMENT OF MATERIALS ENGINEERING, BERLIN, GERMANY

Correspondence address: radzisze@agh.edu.pl

TABLE 1
Chemical composition of the examined stainless steel exposed for 5 h to Ar-SO_2 atmosphere at 600 °C

Element, %	C	Si	Mn	Cr	Ni
	0.16-0.25	≤0.8	≤0.8	12-14	≤0.6

The corrosion scale appeared after high-temperature corrosion on the Fe-Cr alloy surface. To determine the type of growing phases, the microstructure and the changes of elements distribution in corroded layers, the scanning and transmission electron microscopy (SEM, TEM, HRTEM, STEM) and energy dispersive spectroscopy (EDS) were applied. The examination of scale microstructure and chemical composition were performed with the SEM (FEI Inspect S50 and FEI Nova NanoSEM 450) and the TEM (JEM 2200FS-Jeol), operating at the acceleration voltage of 200 kV and equipped with an energy dispersive X-ray spectrometer (EDS) and an in-column omega-type energy filter [18-19]. The samples for TEM observations were cut with a focused ion beam along the normal to the surface of the corroded layer. An electron-transparent lamella was extracted from bulk specimen by the in- situ lift-out (INLO) method. Before cutting the area of interest, a Pt line was deposited. The Pt line was used to protect the top area of the specimen, to ensure better electrical contact and to mark the position of the target area [18-19]. Detailed analyses of representative areas were performed to deduce more spatial information about the scale phase composition. Fast Fourier transform (FFT) was used to get an analogue of electron diffraction patterns for zone axis identification. The phase identification operations were supplemented by a TEM-EDS analysis. The energy-filtered TEM (EFTEM) measurements were carried out to acquire proper differentiation of chromium and oxygen presence.

3. Results and discussion

Oxide-sulfide scales can form on commonly used materials, like Fe alloys, in oxygen and sulphur-containing atmospheres [13-17]. The presented results concern the early stage of the scale growth. In the text, the terms “scale” and “corroded layer” are used interchangeably. SEM observations showed that the thin scale was formed after high-temperature corrosion of X20Cr13 steel (Fig. 1). As shown in Fig. 1, scale was not uniformly homogeneous in structure.

The obtained thin scale was compact and adhered well to the steel surface. The exposure to Ar-SO_2 atmosphere at 600 °C for 5 h caused rapid nucleation and growth of Fe, Cr and Mn oxides. For some time, this growing thin scale can give protection for the base material, even when the crystalline layer expands as a result of further corrosive process.

SEM micrographs obtained from the scale surface showed that the scale exhibited the signs of grain boundaries from the underlying metal substrate (Figs. 1-2). However, EDS elements mapping analysis of the corroded layer surface revealed the appearance of iron and chromium oxides. The observed grain boundaries were richer in chromium, carbon and the contact with the corrosive environment caused oxidation of these phases (Figs. 1-2).

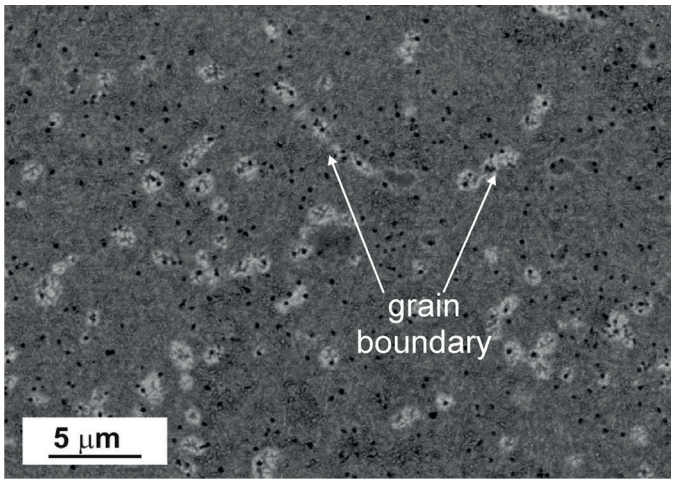

Fig. 1. SEM-BSE image of the surface of X20Cr13 steel exposed to Ar-SO_2 atmosphere at 600 °C for 5 h

While this was shown by the energy dispersive spectroscopy, these areas revealed lower concentration of iron and manganese. As other researchers reported [20-23], components can be expected on the scale surface SO_x. Some authors [23] reported that the $Fe_{1-x}S$ phase formed on the surface of Fe-Cr alloy (up to 2 at.% Cr). On the other hand, within the range of 2-40 at.% Cr, the scale composed of heterophasic mixture of $Fe_{1-x}S$ and spinel $FeFe_{2-x}Cr_xS_4$ [23]. Kamel et al. [24] showed that $Fe_{1-x}S$, chromium oxide and nickel sulphide can exist on the surface of 304L stainless steel (Fe-18Cr-8Ni (wt. %)) exposed to an atmosphere containing high amounts of sulphur at 300 °C. However, Figure 2 shows that sulphur is uniformly distributed and sulphides were not formed. Numerous researches have shown that the growth of the corroded layer on Fe alloy occurs by outward diffusion of metal ions and electrons through lattice defects [20-21]. In addition, the process of iron sulphurization proceeds in accordance with the parabolic rate law. The slowest partial process defining the corrosion rate is outward diffusion of Fe ions through singly-ionized cation vacancies [13, 20-21]. The authors also confirmed (by XPS analysis) the appearance of Cr, Fe and Mn on the scale surface. The TEM bright-field image in Figure 3 shows the cross-section of the corroded layer. The scale thickness varied from 30 nm to 80 nm. This layer consists of three zones (Fig. 4a and c).

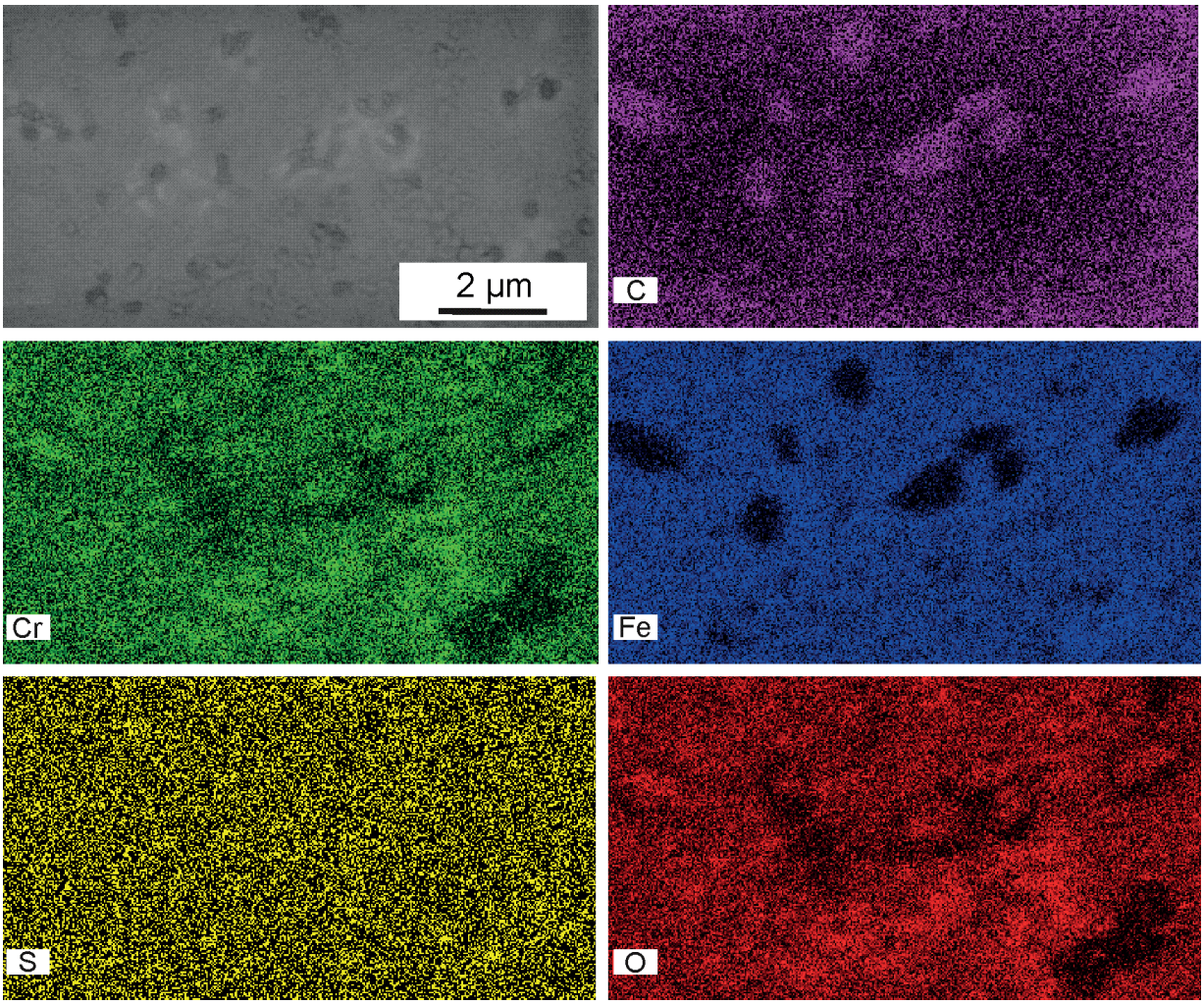

Fig. 2. SEM image and EDS mapping of the surface of X20Cr13 steel exposed to Ar-SO_2 atmosphere at 600 °C for 5 h

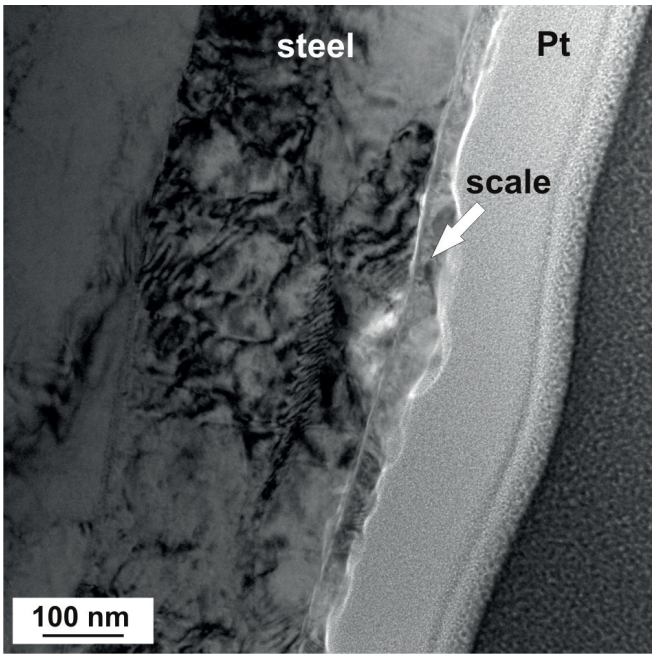

Fig. 3. TEM bright-field image of the scale, obtained after high-temperature sulphide corrosion at 600 °C for 5 h (cross-section); Pt-protection layer deposited on the sample surface

Zone 1 grew at the beginning of the high-temperature process and its thickness varied from 1 nm to 3 nm (Fig. 4b). This region had an amorphous microstructure (Fig. 4b). Zone 2 possessed a nanocrystalline structure. The thickness of this zone varied within the range of 1-2 nm. Subsequently, further interaction of the corrosive environment with the steel surface resulted in the growth of larger grains (zone 3) (Fig. 4b). The HRTEM studies made it possible to distinguish the atomic planes of the formed scale. The observations demonstrated differences in the dimensions of crystallites. At the beginning of the corrosion process, grains with the size from 5 nm up to 8 nm were formed (Fig. 4c). In the second nanostructured zone, the crystallites were clearly smaller than in zone 3 (Fig. 4b). Further heating and influence of aggressive atmosphere resulted in the growth of grains that were more than 30 nm in size. Locally, the orientation transfers in some areas to the larger crystallites (Fig. 4a-b). The FFT was applied, in order to identify the phase composition (Fig. 5).

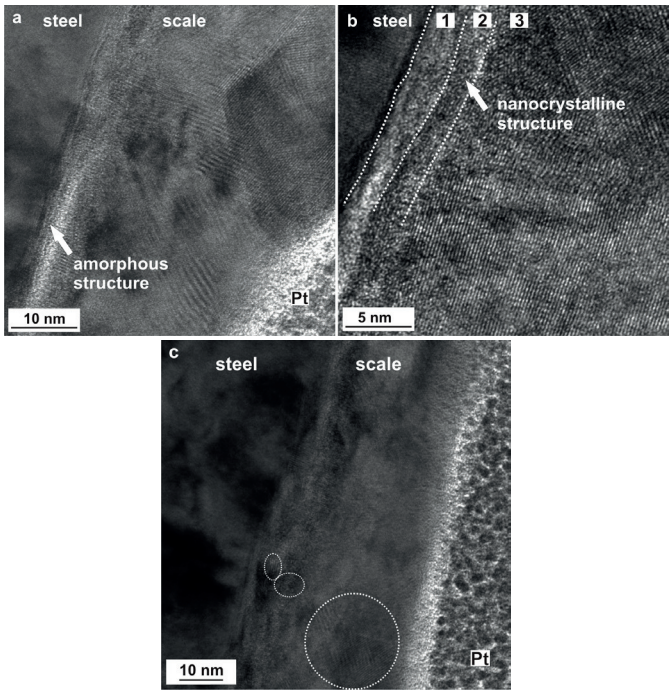

Fig. 4. (a) HRTEM image showing a corroded layer obtained on X20Cr13 steel after high-temperature corrosion caused by exposition to Ar-SO_2 atmosphere at 600 °C for 5 h; (b) HRTEM bright-field image of selected zones of the scale with different microstructures: zone 1 - amorphous, 2 - nanocrystalline, 3 - coarse grains; (c) The scale cross-section (BF-TEM) -selected grains with the different size

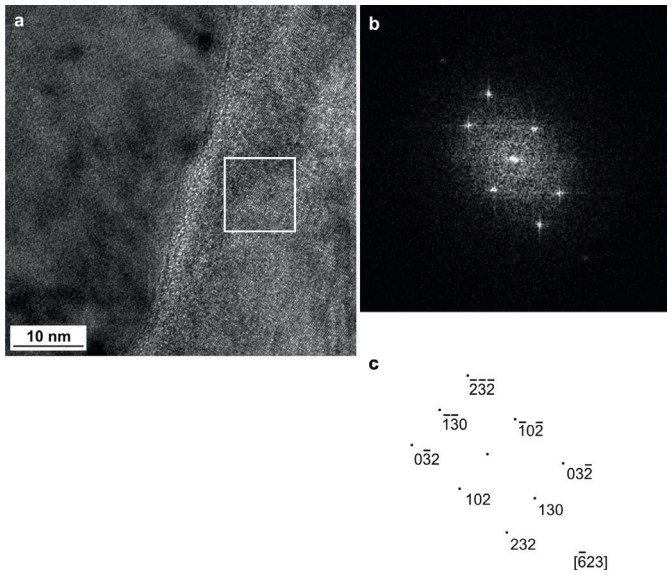

Fig. 5. (a) STEM micrograph of the scale formed during high-temperature corrosion process, proceeding at 600 °C for 5 h in the atmosphere consisting of 0.25 vol.% SO_2 and 99.75 vol.% Ar; (b) fast Fourier transformation (FFT) from the area marked in Fig. 5a; (c) indexed diagram of FFT pattern

An FFT image was taken from the nanocrystalline area that is marked with the square in HRTEM image (Fig. 5). Crystallites corresponding to the reflections on the Fourier transform were visible in the scale. It was found that the diffraction pattern corresponds to Cr_5O_{12} in the [623] zone axis (Fig. 5). However, according to the EDS results, the phase composition could be written as $(Cr, Mn, Fe)_5O_{12}$.

EDS examinations revealed that the elements diffuse from the steel substrate (X20Cr13) into the corroded layer. The investigations also showed a different range of diffusion for each element, which leads to the formation of the inner structure of the scale (Fig. 6). Chromium, manganese and oxygen enrichment was observed at the steel/scale interface.

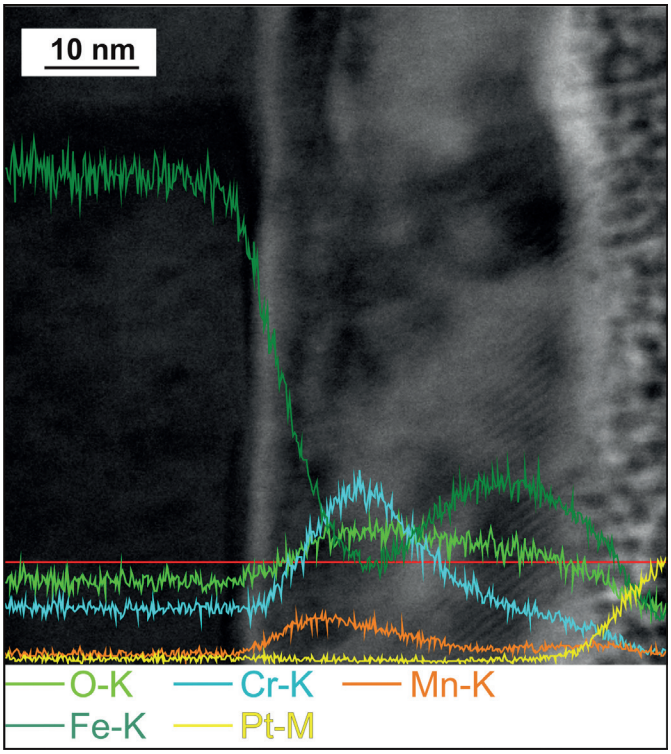

Fig. 6. STEM BF micrograph and linear distribution (TEM-EDS) of Fe, Cr, Mn, O and Pt in the cross-section of the scale obtained after high-temperature corrosion of X20Cr13 steel

Chromium diffused only at the beginning of high-temperature corrosion of the examined steel. As opposed to chromium, iron atoms migrated from the substrate towards the scale surface. Therefore, iron reached higher concentration near the scale surface and behind the chromium-rich zone. While the content of manganese was the highest in the scale cross-section. Earlier investigations performed by other researchers [13, 22-24] showed that sulphur is present in the scale and it can form the sulphides. This research showed that the scale is free of sulphur compounds. It was found out that the partial pressure of sulphur was too low to form the sulphides, when this mixture of gas atmosphere (Ar-SO_2) is used during high-temperature corrosion of X20Cr13 steel. Therefore, from the thermodynamic point of view, sulphides and oxides may form due to a reaction between metal and SO_2 dissociation products, namely oxygen and sulphur, when the partial pressures of oxygen and sulphur are higher than their equilibrium pressures [25]. Additionally, chemical affinity of steel elements with oxygen is considerably higher than with sulphur. Therefore, in sulphur dioxide atmosphere provides conditions for the formation of oxides rather than sulphides [20]. In contrast to these results, oxygen is detectable in the entire scale. EDS findings were acquired by energy filtered TEM (EFTEM) in order to confirm the differentiation of oxygen and chromium (Fig. 7).

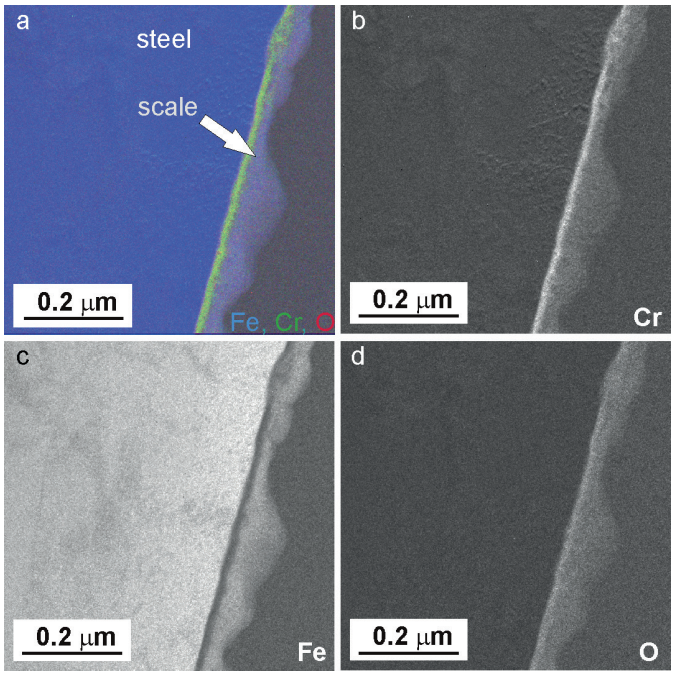

Fig. 7. EFTEM of Cr, O, Fe and the cross-section of the scale formed after high-temperature corrosion proceeding at 600 °C in Ar–SO_2 atmosphere for 5 h

As can be seen in Figure 7, oxygen showed uniform distribution in the cross-section of the scale.

4. Conclusions

SEM and HRTEM studies showed that high-temperature corrosion of X20Cr13 steel in Ar-SO_2 gas mixture led to the formation of a thin corroded layer. The results correspond to the initial growth stage of the corroded layer. Due to low sulphur concentration in the Ar-SO_2 atmosphere sulphides were not formed in the early stage of high-temperature corrosion of the steel surface. Sulphur had a uniform distribution on the surface of chromium steel. The cross-sectional TEM studies showed that the scale consisted of three zones, characterized by different microstructures. First, a zone with an amorphous microstructure was formed. Then nanocrystals started to grow (5-8 nm). The last zone was composed of coarser grains, with the grain size close to 30 nm. It was found that steel elements diffused. Therefore, chromium was in the corroded layer near the steel surface, while iron diffused through the inner layer of the scale up to its surface. The thin corroded layer on the surface of stainless steel consisted of the $(Cr, Mn, Fe)_5O_{12}$ phase.

Acknowledgements

The authors would like to thank BAM for founding. The work was supported also by the Ministry of Science and Higher Education of Poland under contract No. 11.11.110.295

REFERENCES

[1] M. Schulte, A. Rahmel, M. Schütze, Oxid. Met. **49**, 33 (1998).
[2] M. Danielewski, K. Natesan: Oxid. Met. **12**, 227 (1977).
[3] W. Schulz, M. Nofz, M. Feigl, I. Dörfel, R.S. Neumann, A. Kranzmann, Corros. Sci. **68**, 44 (2013).
[4] F. Liu, J. Tang, T. Jonsson, S. Canovic, K. Segerdahl, J. Svensson, M. Halvarsson, Oxid. Met. **66**, 295 (2006).
[5] S. Jianian, Z. Longjiang, L. Tiefan, Oxid. Met. **48**, 347 (1997).
[6] V. Lepingle, G. Louis, D. Allué, B. Lefebvre, B. Vandenberghe, Corros. Sci. **50**, 1011 (2008).
[7] A. Ruhl, A. Kranzmann, Int. J. Greenhouse Gas Control **9, 85** (2012).
[8] K. Strafford, P. Datta, Corros. Sci. **35**, 1053 (1993).
[9] [9] A. Ruhl, A. Kranzmann, Energy Procedia **37**, 3131 (2013).
[10] R. Niccole, A. Rist: Metall. Trans. B **10B, 429** (1979).
[11] A. Hansson, M. Burriel, G. Garcia, S. Linderoth, M. Somers, Oxid. Met. **68**, 23 (2007).
[12] M. Pillis, L. Ramanathan, Mater. Res. **7**, 97 (2004).
[13] S. Mrowec, K. Przybylski, High Temp. Mater. Proc. **6**, 1 (1984).
[14] R. Lobnig, H. Schmidt, K. Hennesen, H. Grabke, Oxid. Met. **37**, 81 (1992).
[15] J. Hucińska, Adv. Materials Sc. **6**, 16 (2006).
[16] N. Folkeson, L.-G. Johansson, J.-E. Svensson, J. Electrochem. Soc. **154**, C515 (2007).
[17] J. Smith, O. Van der Biest, J. Corish, Oxid. Met. **24**, 277 (1985).
[18] M. Ritter, A landmark-based method for the geometrical 3D calibration of scanning microscopes, Berlin 2007.
[19] I. Dörfel, H. Rooch, W. Österle, Thin Solid Films **520**, 4275 (2012).
[20] P. Marcus, Corrosion Mechanisms in Theory and Practice, New York 2002.
[21] S. Mrowec, Oxid. Met. 44, 177 (1995).
[22] T. Narita, K. Nishida, Oxid. Met. 6, 157 (1973).
[23] S. Mrowec, T. Weber, T. Walec, Oxid. Met. 1, 93 (1969).
[24] M.E. Kamel, A. Galtayries, P. Vermaut, B. Albinet, G. Foulonneau, X. Roumeau, B. Roncin, P. Marcus, Surf. Interface Anal. 42, 605 (2010).
[25] I. Barin, O. Knacke, O. Kubaschewski, Thermochemical Properties of Inorganic Substances, Springer-Verlag, Berlin (1977).